




Decreased brain functional connectivity is associated with faster responses to repeated visual stimuli

Anna Boronina^{1,a}, Vladimir Maksimenko^{1,2,b}, Artem Badarin^{2,c}, and Vadim Grubov^{2,d} 

¹ Innopolis University, 1 Universitetskaya, Innopolis 420500, The Republic of Tatarstan, Russia

² Baltic Center for Neurotechnology and Artificial Intelligence, Immanuel Kant Baltic Federal University, 14 A. Nevskogo, Kaliningrad 236016, Russia

Received 16 May 2024 / Accepted 2 August 2024

© The Author(s), under exclusive licence to EDP Sciences, Springer-Verlag GmbH Germany, part of Springer Nature 2024

Abstract When processing repetitive visual stimuli, the brain experiences neuronal adaptation, a process that reduces its response time by pre-activating specific neural groups crucial for handling these stimuli. While prior research has extensively examined this phenomenon within distinct brain regions, the interactions between these regions during adaptation have remained less understood. In this study, we explored these inter-regional interactions by assessing functional connectivity using the phase locking value. Our analysis showed a reduction in functional connectivity both within the occipito-parietal region and between occipito-parietal and central regions as time spent on task increased. Interestingly, these changes in connectivity were positively correlated with shorter processing times for these stimuli. To determine whether these connectivity changes could be attributed to increasing fatigue, we also measured the amplitude–velocity ratio of blinks. Our results revealed no significant correlation between this indicator of fatigue and the observed shifts in connectivity. This suggests that the noted alterations in functional connectivity are more likely related to neuronal adaptation mechanisms, rather than merely reflecting changes in fatigue levels as detected through EEG signals.

1 Introduction

Synchronization between neurons is the basis of operation in the neural network of brain. This synchronization underlies the interaction between neural ensembles, a phenomenon known as functional connectivity [1]. Functional connectivity can show two types of patterns. First, there is segregation, where certain brain regions demonstrate strong synchronization within their own groups of neurons, but have weaker connections between brain regions. Second, there is integration, synchronous patterns with global properties, where connections are stronger between neuronal populations from different brain areas [2, 3].

Neurophysiological findings show that neurons synchronize through low-frequency rhythms, such as theta (4–8 Hz), alpha (8–12 Hz), and beta (15–30 Hz). Despite neurons firing electrical impulses (spikes) at high frequencies, up to 100 Hz, these spikes are effectively relayed from one neuron (presynaptic) to another (post-synaptic) with the help of low-frequency modulation [4]. For a connection between two neurons to occur, spikes from the presynaptic neuron need to align with the excitability cycle of the post-synaptic neuron. To facilitate this transmission, low-frequency rhythms modulate the activity of these neurons [5]. Consequently, these low-frequency components become noticeable in the spectrum of neuronal activity across different neural populations. Phase relations between these components hold valuable information about how synchronized these neural populations are.

The low-frequency patterns can be detected by noninvasive electroencephalography (EEG). EEG sensors gather summarized signals from millions of neighboring neurons in the area of recording electrode. The power spectra of EEG signal typically show peaks in specific frequency ranges, matching the rhythms mentioned earlier. This indicates that large numbers of neurons contribute to these spectral components. The stronger and sharper these

^a e-mail: annwhoorma@gmail.com

^b e-mail: maximenkovi@gmail.com

^c e-mail: badarin93@gmail.com

^d e-mail: vvgrubov@gmail.com (corresponding author)

peaks are, the more synchronized the neurons are within that rhythm. By examining EEG signals from different areas of the cortex and studying the phase relations of the low-frequency components, we can assess the extent of neurons' synchronization in these areas. This estimation helps us understand how effectively the neurons exchange signals [6, 7].

In this context, phase locking value (PLV) is commonly used in research to uncover how neurons interact. This method builds upon the results found through spectral power analysis [8]. PLV helps to shed light on various brain activities, such as visual processing [9], motor functions [10], and sleep stages [11]. PLV is also used to create features that help distinguish between different emotional states [12] and types of movement [13]. Moreover, PLV is a powerful tool for identifying EEG markers for neurological conditions like epilepsy [14], depression [15], and Parkinson's [16].

In our study, we use this metric to understand how the brain network behaves during a prolonged task involving the interpretation of the repeatedly presented similar visual stimuli. Previous research suggests that when the same or similar stimulus is shown repeatedly in short time-intervals, the brain becomes quicker at processing it [17]. Initially, this phenomenon was explored through examining local changes in brain activity. Studies revealed that as time passes during the task, the brain anticipates and prepares certain groups of neurons that will be involved in processing of the upcoming information. As a result, it takes less time for these groups of neurons to engage when processing the next stimulus [18].

The specific network properties contributing to this effect are still not fully understood, although studies report the vital role of neural interactions in visual information processing [19]. During processing of stimuli, brain activity involves a coordinated interaction among various regions [3, 20]. In the case of visual processing, this entails a series of complex steps, starting with initial visual processing in the occipital areas, followed by higher level interpretation in the frontal regions, and culminating in the execution of motor responses by neural populations in the motor areas. Therefore, we expect that the brain modulates the interactions between these distinct regions to maintain the performance of visual processing over an extended task duration [21, 22].

Finally, when engaged in prolonged tasks involving information processing, respondents may exhibit increasing mental fatigue, resulting in decreased performance and diminished neural activity in different areas and frequency bands [23, 24]. Therefore, it is intriguing to determine if fatigue also induces changes in functional connectivity, and if so, to distinguish between changes caused by the fatigue and implemented by the brain to maintain performance during prolonged tasks.

To address these issues, the study aims to test four hypotheses. First, we examine if the response time, which we consider a measure of performance, decreases with time spent on the task. Second, we check if the amplitude–velocity ratio of blinks, which we regard as an indicator of fatigue, increases with the time spent on the task. Third, we anticipate changes in functional connectivity between and within different EEG sensor areas as the experiment progresses. Fourth, we explore whether the changes in functional connectivity are correlated with observed changes in the response time and the amplitude–velocity ratio of blinks.

2 Materials and methods

2.1 Participants

Twenty-one healthy subjects (seven females) aged 18–26 years ($M = 18.9$, $SD = 1.9$) with normal or corrected-to-normal visual acuity participated in the experiment. All of them provided written informed consent in advance. All participants were naïve. The study was approved by the local Ethics Committee and was following the Declaration of Helsinki, except for registration in a database.

2.2 Visual stimuli

We selected an ambiguous 2D representation of a Necker cube as our bistable visual stimulus [25–27]. To a subject without perceptual abnormalities, this 2D image can appear as a left- or right-oriented 3D object. The ambiguity and orientation of the 3D cube is defined by the balance in brightness of the inner edges that form left-lower ($b_l = 1 - a$) and right-upper ($b_r = a$) intersections in the 2D image, where $a \in [0, 1]$ represents a normalized edge's luminance in a grayscale palette [28, 29].

In our experiment, we used a series of Necker cube images with a values taken from the set $\{0.15, 0.25, 0.4, 0.45, 0.55, 0.6, 0.75, 0.85\}$ (Fig. 1A). This set could be categorized into subsets of left-oriented $a = \{0.15, 0.25, 0.4, 0.45\}$ and right-oriented cubes $a = \{0.55, 0.6, 0.75, 0.85\}$. Alternatively, the set could also be divided into low-ambiguity (LA) images $a = \{0.15, 0.25, 0.75, 0.85\}$, easily interpreted by an observer, and high-ambiguity (HA) images $a = \{0.40, 0.45, 0.55, 0.60\}$, which require more cognitive effort for interpretation. Similar to our

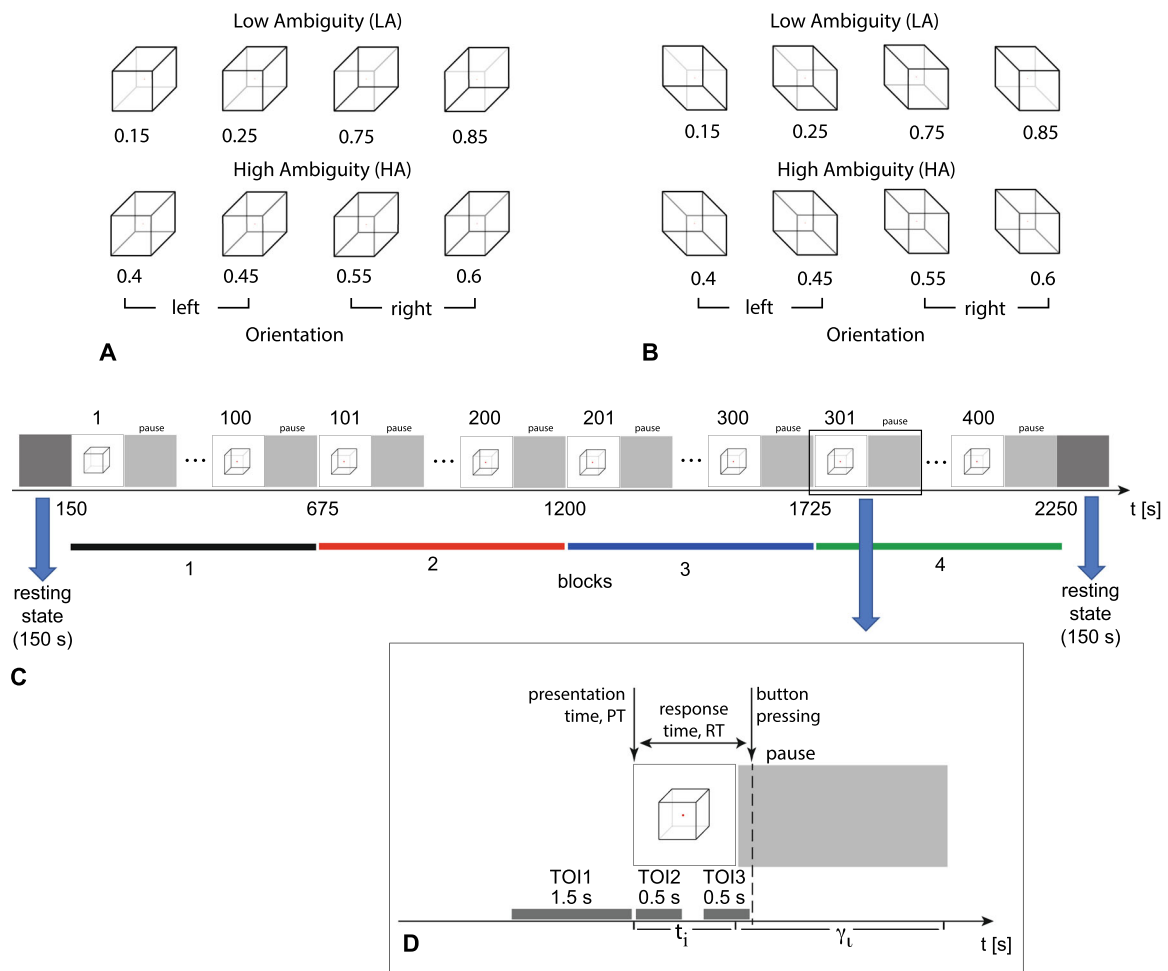


Fig. 1 The set of visual stimuli includes Necker cubes, showcasing both the classical drawing (A) and the mirrored drawing (B). Each set consists of cubes categorized into low ambiguity (LA) on the top row and high ambiguity (HA) on the bottom row. Based on spatial orientation, these cubes are further divided into left-oriented and right-oriented. Experimental session (C) includes the resting state recordings and presentation of 400 stimuli divided into four blocks each including 100 stimuli. Each stimulus presentation (D) lasts for $\tau_i \in [1, 1.5]$ s and is followed by the $\gamma_i \in [3, 5]$ s pause. The TOI1 represents the 1.5 s time interval preceding the stimulus presentation, TOI2,3—0.5 s intervals following the stimulus onset and preceding the button press, respectively

recent study [30], all stimuli were mirrored horizontally. The task involved 16 stimuli (Fig. 1A, B): eight cubes with different contrasts of the inner edges, presented with two possible orientations, classical and mirrored.

There were two main reasons to choose the Necker cube for this study. First, it is a bistable image and, thus, the stimulus has only two possible interpretations. This results in a simple classification task, which is more suitable for repeated visual stimuli experiment. Second, the ambiguity of the stimuli can be controlled with parameter a , and this allows to introduce the complexity of the task. Variations in the task, including its complexity, help to keep the subject involved during the prolonged experiment.

2.3 Experimental procedure

Necker cubes of 22.55×22.55 cm were displayed on a white background using 24" monitor (52.1×29.3 cm) with 1920×1080 resolution and 60 Hz refresh rate. Participants were seated ~ 80 cm away from the monitor, resulting in a visual angle of ~ 0.39 radians. For each participant, experiment lasted approximately 40 min, including 150 s EEG recordings of eyes-open resting state before and after the main experiment (Fig. 1C).

Necker cubes with predefined a -values (selected from the set shown in Fig. 1A, B) were randomly presented 400 times during the experimental session. Each cube with a specific ambiguity appeared approximately 50 times. The presentation time interval τ_i for each stimulus ranged from 1 to 1.5 s. The pauses between consecutive presentations of the Necker cube images, γ_i , ranged from 3 s to 5 s, and these intervals contained an abstract image demonstration,

represented by the white noise picture. The stimulation session was divided into four consecutive blocks, each lasting 10 min and comprising the presentation of 100 stimuli (see Fig. 1C). Participants were instructed to determine the orientation of the Necker cube (defined by a) and press the corresponding button (left or right) on the joystick. Using their responses, we calculated the response time (RT) as the duration between the stimulus onset and button press. For each respondent, we averaged RT across the stimuli belonging to each block resulting in the four RT values per respondent. In this study we regarded RT as a measure of task's performance. Another metric, that could possibly be used for this, is the percentage of correct answers. However, in the current study, this metric was universally high across all subjects (more than 95%), and thus, it was deemed unrepresentative.

2.4 EEG recording and processing

We captured EEG data using 64 electrodes placed according to the "10–10" system at a sampling rate of 1 kHz. The "TP10" electrode served as the reference channel. Our data acquisition utilized actiCHamp amplifier from Brain Products. Prior to analysis, the data underwent preprocessing to remove various biological artifacts. To eliminate oculomotor artifacts, we employed the independent component analysis (ICA) within the MNE Python software package [31]. Specifically, we utilized the "FastICA" algorithm described in Hyvärinen's work [32] to extract the oculomotor component. To optimize the FastICA method's efficacy, we preprocessed the EEG signal by applying finite impulse response (FIR) filters, targeting the removal of low-frequency drift and high-frequency noise within the 1–40 Hz frequency range. After preprocessing, we segmented the EEG signals into 4-s trials, each corresponding to a single Necker cube presentation. These trials included a 2-s interval before and after the demonstration of the stimulus, as well as the response period, featuring a 2-s interval before and after the button press. Finally, we defined three specific time-intervals of interest (TOI): TOI1—1.5 s preceding the stimulus presentation (cube); TOI2—0.5 s following the stimulus presentation; TOI3—0.5 s preceding the button press (see Fig. 1D).

2.5 Graph construction from EEG data

We computed functional connectivity between EEG signals using PLV, as outlined in [33]. We utilized the PLV equation $PLV = |E[S_{xy}/(|S_{xy}|)]|$, where $E[\]$ —time averaging, S_{xy} —cross-spectral power density between two EEG time series $x(t)$ and $y(t)$ [34], $|S_{xy}|$ —absolute value of the cross-spectral power density used for normalizing phase connectivity. We used a multitaper spectral estimation method [35, 36], and the cross-spectral density was computed separately for each taper and aggregated using a weighted average, where the weights correspond to the concentration ratios between the Discrete Prolate Spheroidal Sequences (DPSS) windows.

The MNE software package [31] was employed for these calculations. Connectivity analysis was performed on EEG data collected for each time interval of interest within three frequency ranges: theta-band (4–8 Hz), alpha-band (8–13 Hz), and beta-band (15–30 Hz). The results were organized as a 64×64 connectivity matrix, indicating PLV for all pairs of EEG signals. Across subjects, PLV values within these matrices were averaged across 100 stimuli presented in blocks 1–4. Given the nature of an undirected graph, we focused solely on the lower half of this matrix, situated below the main diagonal (Refer to Fig. 2A).

The EEG sensors were grouped into five spatially neighboring sets (as shown in Fig. 2C). We delineated five regions of interest: frontal (F), left temporal (TL), central (C), right temporal (TR), and occipito-parietal (OP). The choice of the regions of interest is supported by our recent findings regarding top-down and bottom-up mechanisms in processing of the Necker cube [18]. For clear representation, the matrix elements were arranged, so that those corresponding to a specific area were clustered together, allowing us to partition the matrix into these five regions (Fig. 2A). Subsequently, we determined both within-region and between-region connectivity. Within-region connectivity was computed by averaging PLV across pairs of EEG signals captured by sensors within a specific area. For example, to calculate within-region connectivity for the occipital and frontal regions, PLV were averaged across areas 1 and 2 of the matrix (highlighted by yellow triangles). On the other hand, between-region connectivity for a pair of regions involved averaging PLV across all pairs of EEG signals recorded within those respective areas. For instance, calculating connectivity between occipito-parietal and frontal regions required averaging PLV across area 3 of the matrix (highlighted by the blue rectangle).

2.6 Amplitude–velocity ratio of blinks

Our chosen indicator of fatigue, amplitude-velocity ratio of blinks (AVR), is calculated based on electrooculogram (EOG). Since our experimental setup did not include EOG recording, we extracted EOG from EEG data. For this, we again employed a methodology based on decomposing EEG signals into independent components. We decomposed the original EEG dataset into independent components, selecting the component associated with eye movements (EOG signal) based on z -score estimation [37]. From the obtained EOG signal, we identified blinks and computed the ratio of blink amplitude to peak blink closure velocity, serving as an indicator of fatigue. This metric was initially introduced by Johns [38] and quantifies the level of fatigue. Subsequently, AVR values were

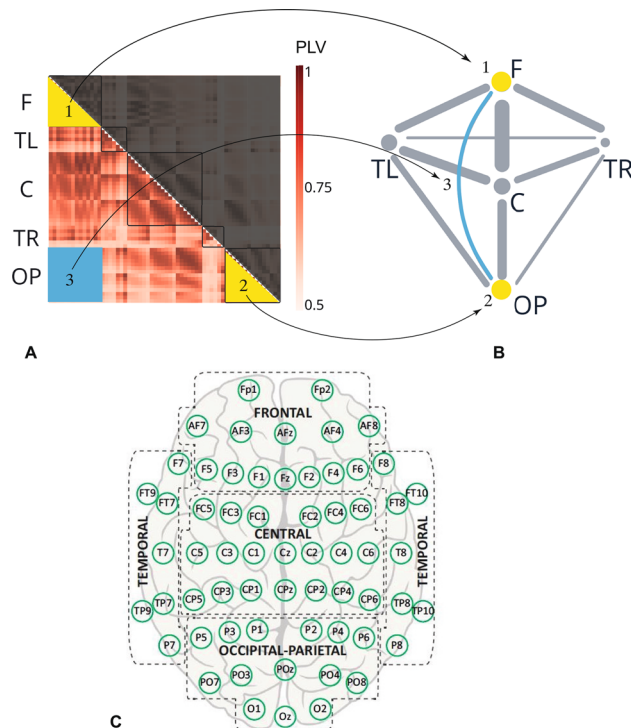


Fig. 2 The connectivity matrix (**A**) displays the PLV for all pairs of EEG signals categorized into 5 regions: frontal (F), left temporal (TL), central (C), right temporal (TR), and occipito-parietal (OP). Graph (**B**) represents connections both within and between these regions, based on PLV. The lines signify the connections between nodes belonging to these different regions, with their width indicating the average PLV across all connections between nodes belonging to these different regions. The circles represent connectivity within regions. The circle size corresponds to the average PLV across connections between nodes within that region. Scheme (**C**) illustrates EEG sensors belonging to each region

averaged across blocks 1–4 for each subject. We utilized the MNE software package [31] to extract the EOG from the EEG data. For blink detection and calculation of their characteristics, we employed the neurokit2 Python software package [39].

2.7 Correlation analysis

To find a correlation between the behavioral metrics and functional connectivity, we used repeated-measures correlation. Repeated-measures correlation (RMC) is a statistical technique used to examine the relationship between two variables when both variables are measured repeatedly on the same individuals. RMC extends the traditional Pearson correlation to account for the within-subject correlation structure [40]. We performed correlation analysis in Python using pingouin package.

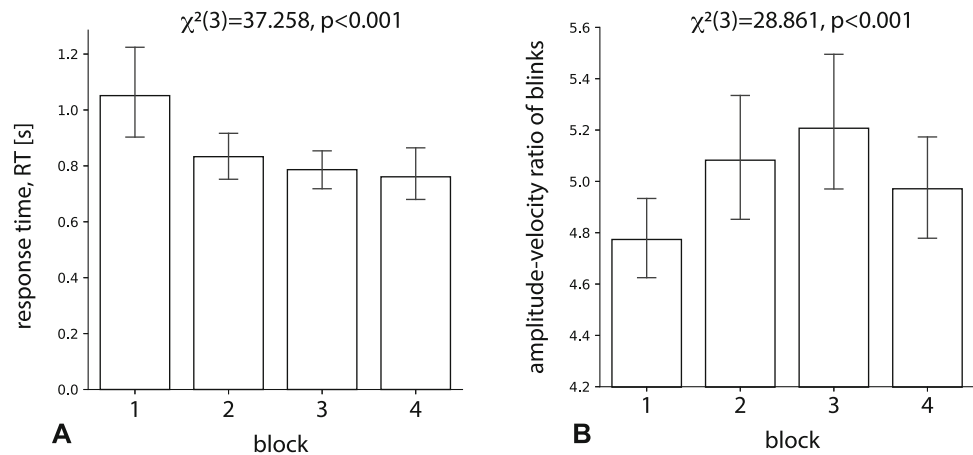
3 Results

3.1 Behavioral metrics

We compared RT between four blocks using nonparametric Friedman test. As a result, we found that RT changed significantly across blocks: $\chi^2(3) = 37.258$, $p < 0.001$. The direction of change is shown in Fig. 3A. RT takes maximal value ($M = 1.051$ s, $SD = 0.381$) in the block 1. In the block 2, RT decreases to ($M = 0.832$ s, $SD = 0.208$). In the block 3 and block 4, RT takes even lower values ($M = 0.786$ s, $SD = 0.165$) and ($M = 0.761$ s, $SD = 0.213$), respectively.

We compared the AVR between four blocks using nonparametric Friedman test. As a result, we found that this metric changed significantly across blocks: $\chi^2(3) = 28.861$, $p < 0.001$. The direction of change is shown in Fig. 3B. The AVR takes the lowest value ($M = 4.773$, $SD = 0.365$) in the block 1. In the block 2 ($M = 5.082$, $SD = 0.540$)

Fig. 3 RT (A) and AVR (B) for each experimental block. Data are shown as group mean and 95% confidence interval. Significance is estimated using Friedman test



and block 3 ($M = 5.207$, $SD = 0.621$), we observe an increase of this value. Finally, it decreases at block 4 ($M = 4.971$, $SD = 0.480$).

3.2 Functional connectivity

We conducted a comparison of within- and between-region PLV across blocks using the nonparametric Friedman test. To account for multiple comparisons, the alpha-level was adjusted to 0.0025. Initially, we assessed PLV calculated in the interval preceding the stimulus presentation (TOI1). Our findings indicated significant PLV changes across two regions: occipito-parietal (OP) region in the theta-band: $\chi^2(3) = 17.971$, $p < 0.001$, and central (C) region in the alpha-band: $\chi^2(3) = 14.2$, $p = 0.002$. Moreover, PLV between these regions in the theta-band changed significantly across blocks: $\chi^2(3) = 18.885$, $p < 0.001$, as highlighted in Fig. 4A (marked in red).

When considering the direction of change, we observed the following trends. In the occipito-parietal area, theta-band PLV reached its peak value ($M = 0.925$, $SD = 0.020$) in block 1. This decreased to ($M = 0.916$, $SD = 0.023$) in block 2, further reducing in blocks 3 ($M = 0.915$, $SD = 0.022$) and block 4 ($M = 0.914$, $SD = 0.025$) (Fig. 4B). Within the central region, alpha-band PLV attained its maximum in block 4 ($M = 0.910$, $SD = 0.018$). It decreased from block 4 to block 3 ($M = 0.904$, $SD = 0.018$), and from block 3 to block 2 ($M = 0.900$, $SD = 0.020$). Finally, for block 1, PLV was ($M = 0.903$, $SD = 0.017$) (Fig. 4C). Regarding theta-band PLV between occipito-parietal and central regions, the maximal value occurred in block 1 ($M = 0.800$, $SD = 0.028$). This declined to ($M = 0.789$, $SD = 0.034$) in block 2, ($M = 0.787$, $SD = 0.033$) in block 3, and stabilized at ($M = 0.789$, $SD = 0.034$) in block 4 (Fig. 4D).

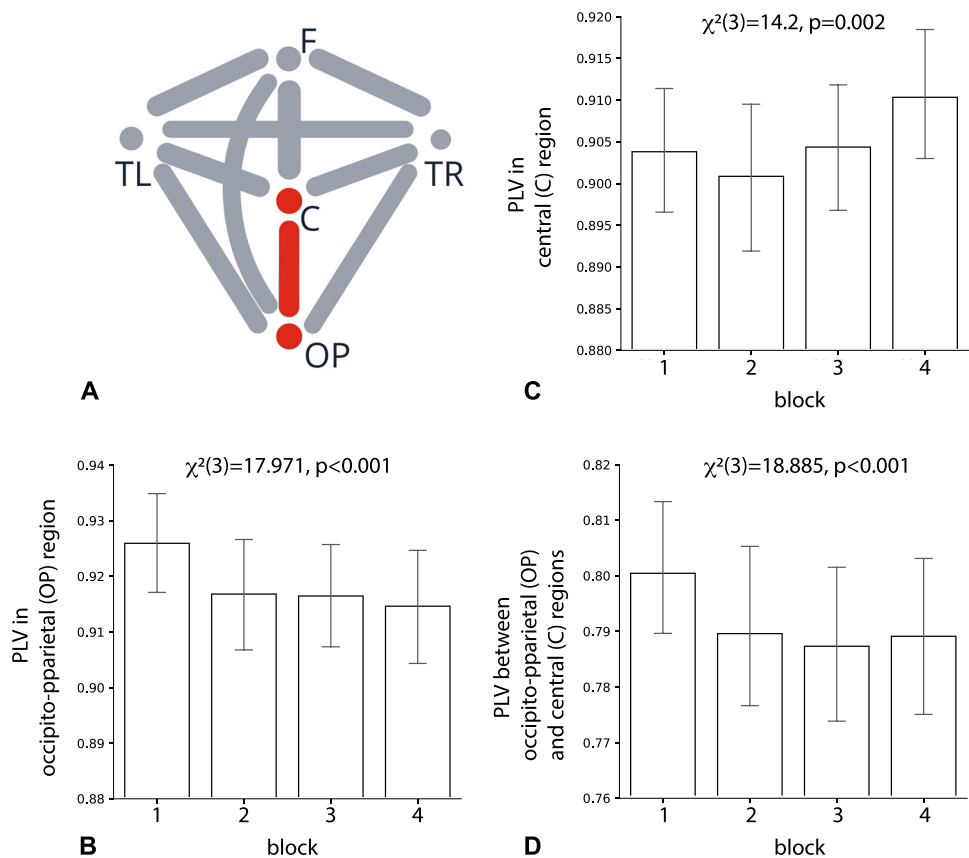
Finally, no statistically significant differences were observed between blocks when considering PLV in the time-intervals following the stimulus presentation (TOI2) or preceding the response (TOI3).

3.3 Correlation between behavioral metrics and functional connectivity

We analyzed correlation between behavioral metrics including RT and AVR and PLV in the theta-band in the parietal region, alpha-band in the central region, and theta-band between central and parietal regions using RMC analysis. We adjusted alpha-level to 0.01 to account for multiple hypothesis testing. The results of correlation analysis are shown in Fig. 5, where dots of different color show data of different respondents and all lines have the same slope fitted to the data.

Correlation analysis revealed several findings. First, we observed a moderate positive correlation between RT and PLV in the theta-band in the parietal region: $r(62) = 0.441$, $p < 0.001$. This indicates that the decrease in RT between blocks is associated with decreasing functional connectivity among neuronal populations in the parietal region (Fig. 5A). Second, no correlation was observed between RT and PLV in the alpha-band in the central region: $r(62) = -0.116$, $p = 0.357$. This suggests no association between decreasing RT between blocks and changes in the functional connectivity among neuronal populations in the central region (Fig. 5B). Third, we observed a moderate positive correlation between RT and PLV in the theta-band between central and parietal regions: $r(62) = 0.441$, $p < 0.001$. This indicates that the decrease in RT between blocks is correlated with decreasing functional connectivity between these regions (Fig. 5C). Fourth, we observed weak-to-moderate negative correlation between AVR and PLV in the theta-band in the parietal region: $r(62) = -0.286$, $p = 0.046$. This finding deemed insignificant after adjusting the alpha-level, suggests no association between changes in AVR between blocks and changes in functional connectivity between neuronal populations in this area (Fig. 5D). Fifth, there

Fig. 4 Representation of the graph restored based on the functional connectivity between EEG signals (**A**). Each node corresponds to the EEG sensor region and reflects within-region PLV. Each edge corresponds to the PLV between these regions. Red color marks the regions and between-region edge where PLV changes significantly between four blocks. Bar-plots illustrate the way the PLV changes between blocks: theta-band PLV in the occipito-parietal (OP) region (**B**), alpha-band PLV in the central (C) region (**C**), and theta-band PLV between occipito-parietal and central regions (**D**). Significance is estimated using Friedman test, uncorrected



was no correlation between AVR and PLV in the alpha-band in the central region: $r(62) = -0.134, p = 0.355$. This implies that changes in AVR between blocks do not associate with changes in functional connectivity between neuronal populations in this region (Fig. 5E). Finally, there was no correlation observed between AVR and PLV in the theta-band between central and parietal regions: $r(62) = -0.245, p = 0.088$. This suggests that changes in AVR between blocks do not associate with changes in connectivity between these regions (Fig. 5F).

4 Discussion

In this study, we utilized PLV, a metric analyzing brain connectivity via EEG signals. Our objective was to examine alterations in neural networks, while participants engaged in a prolonged task of perceiving similar visual stimuli, delivered successively in brief intervals. The EEG sensors placed across the scalp were segregated into five spatial zones, and PLV calculations were used to gauge communication strength within and between these zones. We collected and analyzed several metrics: response time (indicative of the speed of stimulus interpretation), the amplitude-velocity ratio of blinks (reflective of fatigue), and EEG connectivity patterns. The experiment was divided into four blocks, each comprising 100 stimuli, to observe behavioral and connectivity metric change over time.

Our studies resulted in several significant observations:

- (i) participants showed improved response times, indicating enhanced stimulus recognition ability;
- (ii) the amplitude-velocity ratio of blinks escalated throughout the experiment;
- (iii) dynamic alterations in brain connectivity patterns were evident, particularly preceding stimulus presentation;
- (iv) in the theta-band, connectivity within the occipito-parietal area was diminished, alongside decreased connectivity between the occipito-parietal and central regions;
- (v) in the alpha-band, there was an increase in within-zone connectivity within the central area;
- (vi) changes in theta-band connectivity correlated with shorter response times, while alpha-band connectivity changes did not.

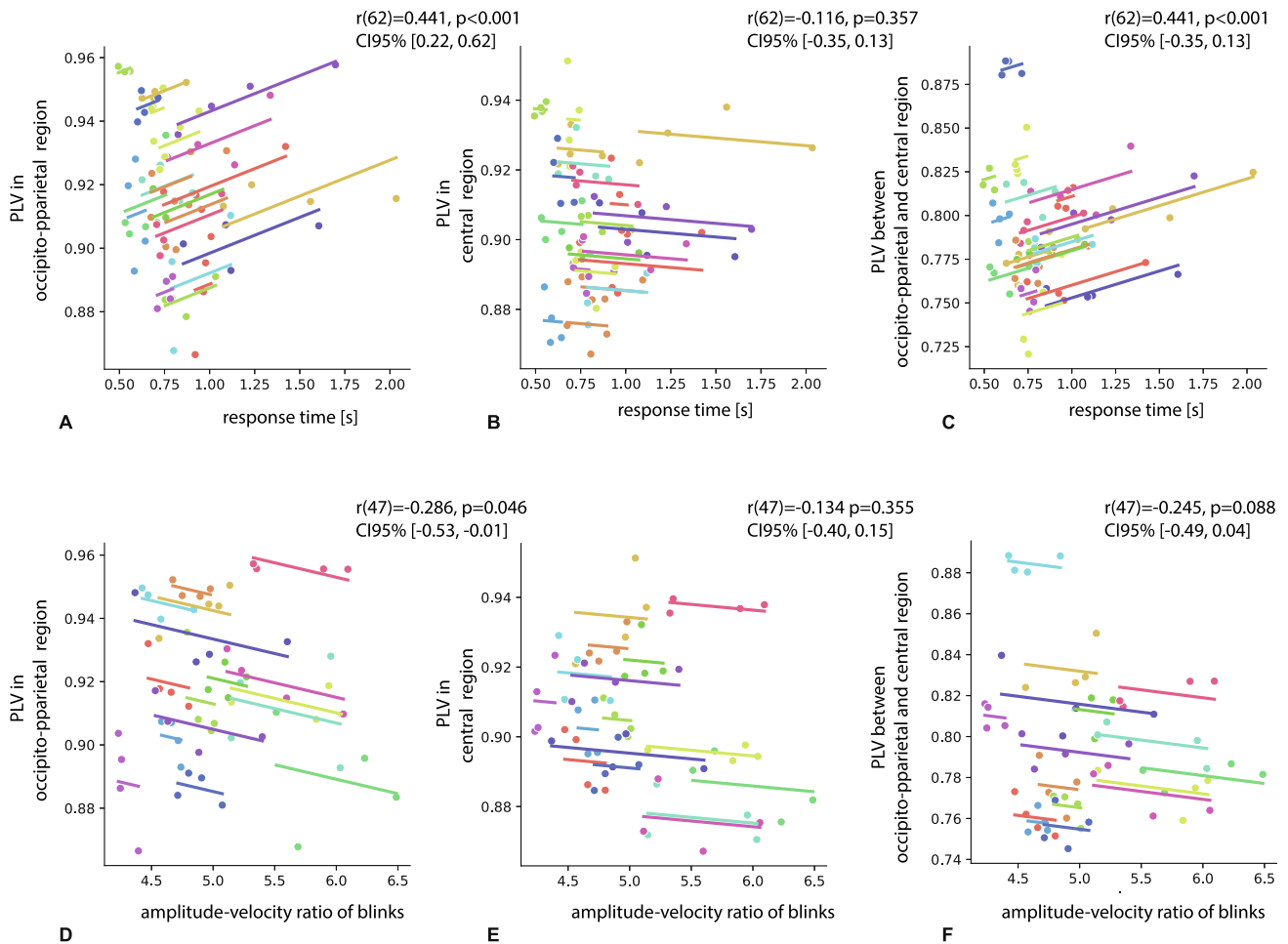


Fig. 5 The top row displays the correlation between RT and PLV in the theta-band in the parietal region (A), the alpha-band in the central region (B), and the theta-band between central and parietal regions (C). The bottom row illustrates the correlation between AVR and PLV in the theta-band in the parietal region (A), the alpha-band in the central region (B), and the theta-band between central and parietal regions (C)

Notably, none of these connectivity patterns aligned with fatigue levels.

Based on these observations, we made the following conclusions.

In tasks involving repeated exposure to similar stimuli, individuals tend to become quicker at processing these stimuli. Our behavioral analysis revealed a 20% reduction in response time from ~ 1 to 0.8 s, aligning with findings from our previous experiments and corroborating similar outcomes from different studies conducted across various laboratories and using different equipment [18, 41]. Additionally, these results align with findings from other researchers, who have reported shorter response times and higher identification rates for repeated stimuli compared to unrepeated ones (for review, see [17]). In our research, despite the shorter response times, accuracy remained consistent throughout the experiment. This indicates that participants made informed decisions rather than randomly pressed buttons, maintaining their accuracy despite the time efficiency.

In prolonged tasks involving repeated exposure to similar stimuli, individuals showed an increase in the amplitude-velocity ratio of blinks, suggesting progressing fatigue. In our study, we utilized a metric known as the amplitude-velocity ratio of blinks, which is proposed as a measure to assess drowsiness levels [38]. This metric is based on the principle that a complete blink lasts for about 100–300 milliseconds in an alert state, and extends beyond 500 milliseconds in a drowsy state due to the eyelids remaining closed longer, presumably because tonic contraction of the orbicularis oculi muscles is inhibited for an extended period. This indicates that blink velocity decreases with drowsiness. It is also established that the velocity of blinks is highly correlated with their amplitude, meaning that the larger the blink, the higher its velocity. However, in states of drowsiness, blinks become relatively slower for a given amplitude. Therefore, a higher amplitude-velocity ratio of blinks indicates increased drowsiness. In our experiment, we observed an approximately 10% increase in the amplitude-velocity ratio of blinks from 4.8 to 5.2, which led us to conclusion that the respondents' fatigue had increased over the course of the experiment.

Changes in the connectivity structure are observed before the stimulus onset, indicating that the brain pre-organizes its structure to prepare for stimulus processing, rather than altering the processing mechanisms themselves. Our results indicate that changes in functional connectivity across the experiment occurred in the pre-stimulus EEG segments. Conversely, there were no changes in functional connectivity within the EEG segments related to stimulus processing and response formation throughout the experiment. This suggests that the brain establishes an optimal connectivity structure beforehand, preparing for effective stimulus processing. These findings align with a recent paper on time–frequency analysis [18] reporting increased spectral power of EEG signals in the time-intervals preceding stimulus presentation in tasks involving the repeated presentation of similar visual stimuli. Furthermore, these results contribute to the fundamental theory of neural adaptation [42]. Neuronal adaptation is known so far as a phenomenon of reduced neuronal response to repeated stimuli compared to un-repeated ones [43]. Its mechanisms have been studied at the single-cell level and at the level of local neuronal ensembles in various brain areas, such as the occipital [44], parietal [45], and frontal [46]. In this respect, our results suggest that neuronal adaptation may manifest at the level of functional networks; the brain may prepare its connectivity structure prior to stimulus onset to reduce the effort of forming functional connections after stimulus onset, thereby reducing the response time needed to process stimuli.

Reduced connectivity in the theta-band within the occipito-parietal region and between the occipito-parietal and central regions correlates with improved stimulus processing speed, rather than fatigue. We observed that decreased phase locking values (PLV) in the occipito-parietal region, as well as between the occipito-parietal and central regions, were associated with shorter response times during the experiment. Notably, there was no correlation between these PLV changes and the amplitude–velocity ratio of blinks, an indicator of fatigue. Another study by Mockel et al. [47] highlights that time-on-task effects are not limited to mental fatigue. Instead, they propose that adaptation during a task influences performance and neurophysiological parameters. Furthermore, they emphasize the importance of considering adaptation when studying time-on-task effects. In line with these findings, our study suggests that the observed changes in neural activity likely reflect adaptation mechanisms. Specifically, we found reduced connectivity in the theta-band within the occipito-parietal region and between the occipito-parietal and central regions, which may indicate neural adaptation to repeated visual stimuli.

Limitations. Our study has few limitations. First, the sample size is small. Power analysis indicates that sample size of 20 participants provides 80% chance of rejecting the null hypothesis at the 5% alpha-level for a large effect size (Cohen's $d > 0.6$). Therefore, future studies with a larger sample size (> 50 participants) are required to capture medium-sized effects.

Second, our study utilizes brain activity signals registered non-invasively from the surface of the skull. As a result, we could not measure the activation of deep brain structures or estimate functional connectivity between them. Meanwhile, a recent study [48] based on fMRI reported that fatigue might also cause decreasing functional connectivity between some regions within the so-called "fatigue network". In our case, we were unable to find a correlation between changes in functional connectivity and fatigue. We suggest that using fMRI may help identify functional connectivity structures associated with both fatigue and adaptation and distinguish between them. Additionally, in our work, connectivity was investigated on the sensor level, i.e., EEG channels. We believe that switching to the source level could also help to study functional connectivity between deep brain structures.

Third, we introduced the complexity of visual classification task via ambiguity of the Necker cube. We believe that taking it into consideration can help to reveal some subtle effects in brain functional connectivity. For example, we may theorize that tasks with low and high complexity lead to formation of somewhat different functional networks. However, the design of experimental study and chosen methods of analysis were ill-suited for introduction of complexity as a factor. Thus, the effects of task's complexity remain the scope of the future research.

Fourth, we assessed the subject's fatigue via eyetracking characteristics alone. Eyetracking can provide indicative markers of fatigue; however, amplitude–velocity ratio of blinks was developed with very tired subjects in mind, and such levels of fatigue may be unattainable in our study. Therefore, future studies will implement methods for finer evaluation of fatigue. Additionally, some other modalities can be used for this purpose—for instance, electromyogram (EMG).

Fifth, we used only PLV to assess functional connectivity in brain. In future, we will explore other metrics such as Phase Lag Index or entropy-based measures.

5 Conclusion

We tested whether the brain adjusts its functional connectivity structure to enhance behavioral performance during a prolonged task involving the perception of repeatedly presented similar visual stimuli.

Our results showed that respondents improved their behavioral performance by decreasing response time by more than 10%. We also observed a $\sim 10\%$ increase in the amplitude–velocity ratio of blinks, indicating increased fatigue among the respondents as the experiment progressed. Brain activity analysis revealed reduced connectivity in the theta-band within the occipito-parietal region and between the occipito-parietal and central regions. Importantly,

these connectivity changes were correlated with improved stimulus processing speed rather than fatigue. We suggest that these alterations in functional connectivity represent mechanisms of neuronal adaptation, which the brain employs to enhance the processing of repeatedly presented stimuli.

Acknowledgements The work was supported by the Russian Science Foundation (Grant No. 23-72-10016).

Data Availability The data presented in this study are available on request from the corresponding author.

References

1. K.J. Friston, Functional and effective connectivity: a review. *Brain Connect.* **1**(1), 13–36 (2011)
2. O. Sporns, Network attributes for segregation and integration in the human brain. *Curr. Opin. Neurobiol.* **23**(2), 162–171 (2013)
3. A.E. Hramov, N.S. Frolov, V.A. Maksimenko, S.A. Kurkin, V.B. Kazantsev, A.N. Pisarchik, Functional networks of the brain: from connectivity restoration to dynamic integration. *Phys. Usp.* **64**(6), 584 (2021)
4. J. González, M. Cavelli, A. Mondino, N. Rubido, A.B. Tort, P. Torterolo, Communication through coherence by means of cross-frequency coupling. *Neuroscience* **449**, 157–164 (2020)
5. P. Fries, Rhythms for cognition: communication through coherence. *Neuron* **88**(1), 220–235 (2015)
6. V.A. Maksimenko, A. Lüttjohann, V.V. Makarov, M.V. Goremyko, A.A. Koronovskii, V. Nedaivozov, A.E. Runnova, G. Luijtelaar, A.E. Hramov, S. Boccaletti, Macroscopic and microscopic spectral properties of brain networks during local and global synchronization. *Phys. Rev. E* **96**(1), 012316 (2017)
7. V.A. Maksimenko, A.E. Runnova, N.S. Frolov, V.V. Makarov, V. Nedaivozov, A.A. Koronovskii, A. Pisarchik, A.E. Hramov, Multiscale neural connectivity during human sensory processing in the brain. *Phys. Rev. E* **97**(5), 052405 (2018)
8. M. Demuru, S.M. La Cava, S.M. Pani, M. Fraschini, A comparison between power spectral density and network metrics: an eeg study. *Biomed. Signal Process. Control* **57**, 101760 (2020)
9. S. Phillips, Y. Takeda, A. Singh, Visual feature integration indicated by phase-locked frontal-parietal eeg signals. *PLoS ONE* **7**(3), 32502 (2012)
10. W. Yi, S. Qiu, K. Wang, H. Qi, L. Zhang, P. Zhou, F. He, D. Ming, Evaluation of eeg oscillatory patterns and cognitive process during simple and compound limb motor imagery. *PLoS ONE* **9**(12), 114853 (2014)
11. H. Huang, J. Zhang, L. Zhu, J. Tang, G. Lin, W. Kong, X. Lei, L. Zhu, Eeg-based sleep staging analysis with functional connectivity. *Sensors* **21**(6), 1988 (2021)
12. Z.-M. Wang, Z.-Y. Chen, J. Zhang, Eeg emotion recognition based on plv-rich-club dynamic brain function network. *Appl. Intell.* **53**(14), 17327–17345 (2023)
13. T. Chouhan, N. Robinson, A. Vinod, K.K. Ang, C. Guan, Wavlet phase-locking based binary classification of hand movement directions from eeg. *J. Neural Eng.* **15**(6), 066008 (2018)
14. Z. Ren, Y. Zhao, X. Han, M. Yue, B. Wang, Z. Zhao, B. Wen, Y. Hong, Q. Wang, Y. Hong et al., An objective model for diagnosing comorbid cognitive impairment in patients with epilepsy based on the clinical-eeg functional connectivity features. *Front. Neurosci.* **16**, 1060814 (2023)
15. U. Zuchowicz, A. Wozniak-Kwasniewska, D. Szekeley, E. Olejarczyk, O. David, Eeg phase synchronization in persons with depression subjected to transcranial magnetic stimulation. *Front. Neurosci.* **12**, 1037 (2019)
16. L. Biase, L. Ricci, M.L. Caminiti, P.M. Pecoraro, S.P. Carbone, V. Di Lazzaro, Quantitative high density eeg brain connectivity evaluation in parkinson's disease: The phase locking value (plv). *J. Clin. Med.* **12**(4), 1450 (2023)
17. R. Henson, M. Rugg, Neural response suppression, haemodynamic repetition effects, and behavioural priming. *Neuropsychologia* **41**(3), 263–270 (2003)
18. A.K. Kuc, S.A. Kurkin, V.A. Maksimenko, A.N. Pisarchik, A.E. Hramov, Monitoring brain state and behavioral performance during repetitive visual stimulation. *Appl. Sci.* **11**(23), 11544 (2021)
19. J. Bullier, Integrated model of visual processing. *Brain Res. Rev.* **36**(2–3), 96–107 (2001)
20. V.A. Maksimenko, A.E. Hramov, V.V. Grubov, V.O. Nedaivozov, V.V. Makarov, A.N. Pisarchik, Nonlinear effect of biological feedback on brain attentional state. *Nonlinear Dyn.* **95**(3), 1923–1939 (2019)
21. N.S. Frolov, V.A. Maksimenko, M.V. Khramova, A.N. Pisarchik, A.E. Hramov, Dynamics of functional connectivity in multilayer cortical brain network during sensory information processing. *Eur. Phys. J. Spec. Top.* **228**, 2381–2389 (2019)
22. N. Frolov, M.S. Kabir, V. Maksimenko, A. Hramov, Machine learning evaluates changes in functional connectivity under a prolonged cognitive load. *Chaos* **31**, 10 (2021)
23. B.T. Jap, S. Lal, P. Fischer, E. Bekiaris, Using eeg spectral components to assess algorithms for detecting fatigue. *Expert Syst. Appl.* **36**(2), 2352–2359 (2009)
24. V. Maksimenko, A. Kuc, N. Frolov, S. Kurkin, A. Hramov, Effect of repetition on the behavioral and neuronal responses to ambiguous necker cube images. *Sci. Rep.* **11**(1), 3454 (2021)
25. M. Wang, D. Arteaga, B.J. He, Brain mechanisms for simple perception and bistable perception. *Proc. Natl. Acad. Sci.* **110**(35), 3350–3359 (2013)

26. J. Kornmeier, E. Friedel, M. Wittmann, H. Atmanspacher, Eeg correlates of cognitive time scales in the necker-zeno model for bistable perception. *Conscious. Cogn.* **53**, 136–150 (2017)
27. A.N. Pisarchik, A.E. Hramov, *Multistability in physical and living systems* (Springer, Cham, 2022)
28. A.E. Runnova, A.E. Hramov, V.V. Grubov, A.A. Koronovskii, M.K. Kurovskaya, A.N. Pisarchik, Theoretical background and experimental measurements of human brain noise intensity in perception of ambiguous images. *Chaos Solitons Fract.* **93**, 201–206 (2016)
29. V.A. Maksimenko, A. Kuc, N.S. Frolov, M.V. Khramova, A.N. Pisarchik, A.E. Hramov, Dissociating cognitive processes during ambiguous information processing in perceptual decision-making. *Front. Behav. Neurosci.* **14**, 95 (2020)
30. A. Kuc, V. Maksimenko, A. Savosenkov, N. Grigorev, V. Grubov, A. Badarin, V. Kazantsev, S. Gordleeva, A. Hramov, Studying perceptual bias in favor of the from-above necker cube perspective in a goal-directed behavior. *Front. Psychol.* **14**, 1160605 (2023)
31. A. Gramfort, M. Luessi, E. Larson, D.A. Engemann, D. Strohmeier, C. Brodbeck, L. Parkkonen, M.S. Hämäläinen, Mne software for processing meg and eeg data. *Neuroimage* **86**, 446–460 (2014)
32. A. Hyvarinen, Fast and robust fixed-point algorithms for independent component analysis. *IEEE Trans. Neural Netw.* **10**(3), 626–634 (1999)
33. R. Bruña, F. Maestú, E. Pereda, Phase locking value revisited: teaching new tricks to an old dog. *J. Neural Eng.* **15**(5), 056011 (2018)
34. J.-P. Lachaux, E. Rodriguez, J. Martinerie, F.J. Varela, Measuring phase synchrony in brain signals. *Hum. Brain Mapp.* **8**(4), 194–208 (1999)
35. P.P. Mitra, B. Pesaran, Analysis of dynamic brain imaging data. *Biophys. J.* **76**(2), 691–708 (1999)
36. D.B. Percival, A.T. Walden, *Spectral analysis for physical applications* (Cambridge University Press, Cambridge, 1993)
37. M. Agarwal, R. Sivakumar, Blink: A fully automated unsupervised algorithm for eye-blink detection in eeg signals. In: 2019 57th Annual Allerton Conference on Communication, Control, and Computing (Allerton), pp. 1113–1121 (2019). IEEE
38. M. Johns et al., The amplitude-velocity ratio of blinks: a new method for monitoring drowsiness. *Sleep* **26**, 2 (2003)
39. D. Makowski, T. Pham, Z.J. Lau, J.C. Brammer, F. Lespinasse, H. Pham, C. Schölzel, S.A. Chen, Neurokit2: A python toolbox for neurophysiological signal processing. *Behav. Res. Methods* **2**, 1–8 (2021)
40. J.Z. Bakdash, L.R. Marusich, Repeated measures correlation. *Front. Psychol.* **8**, 456 (2017)
41. V.A. Maksimenko, N.S. Frolov, A.E. Hramov, A.E. Runnova, V.V. Grubov, J. Kurths, A.N. Pisarchik, Neural interactions in a spatially-distributed cortical network during perceptual decision-making. *Front. Behav. Neurosci.* **13**, 220 (2019)
42. C.L. Wiggs, A. Martin, Properties and mechanisms of perceptual priming. *Curr. Opin. Neurobiol.* **8**(2), 227–233 (1998)
43. J. Benda, Neural adaptation. *Curr. Biol.* **31**(3), 110–116 (2021)
44. R.N. Henson, C.J. Price, M.D. Rugg, R. Turner, K.J. Friston, Detecting latency differences in event-related bold responses: application to words versus nonwords and initial versus repeated face presentations. *Neuroimage* **15**(1), 83–97 (2002)
45. Z. Kourtzi, N. Kanwisher, Cortical regions involved in perceiving object shape. *J. Neurosci.* **20**(9), 3310–3318 (2000)
46. L. Naccache, S. Dehaene, The priming method: imaging unconscious repetition priming reveals an abstract representation of number in the parietal lobes. *Cereb. Cortex* **11**(10), 966–974 (2001)
47. T. Möckel, C. Beste, E. Wascher, The effects of time on task in response selection-an erp study of mental fatigue. *Sci. Rep.* **5**(1), 10113 (2015)
48. G. Wylie, B. Yao, H. Genova, M. Chen, J. DeLuca, Using functional connectivity changes associated with cognitive fatigue to delineate a fatigue network. *Sci. Rep.* **10**(1), 21927 (2020)

Springer Nature or its licensor (e.g. a society or other partner) holds exclusive rights to this article under a publishing agreement with the author(s) or other rightsholder(s); author self-archiving of the accepted manuscript version of this article is solely governed by the terms of such publishing agreement and applicable law.